UC San Diego
UC San Diego Previously Published Works

Title

Glycine by MR spectroscopy is an imaging biomarker of glioma aggressiveness.

Permalink

https://escholarship.org/uc/item/95k6h803

Journal

Neuro-Oncology, 22(7)

ISSN

1522-8517

Authors

Tiwari, Vivek
Daoud, Elena V
Hatanpaa, Kimmo J
et al.

Publication Date

2020-07-07

DOI

10.1093/neuonc/noaa034

Peer reviewed

Glycine by MR spectroscopy is an imaging biomarker of glioma aggressiveness

Vivek Tiwari,* Elena V. Daoud, Kimmo J. Hatanpaa, Ang Gao, Song Zhang, Zhongxu An, Sandeep K. Ganji, Jack M. Raisanen, Cheryl M. Lewis, Pegah Askari, Jeannie Baxter, Michael Levy, Ivan Dimitrov, Binu P. Thomas, Marco C. Pinho, Christopher J. Madden, Edward Pan, Toral R. Patel, Ralph J. DeBerardinis, A. Dean Sherry, Bruce E. Mickey, Craig R. Malloy, Elizabeth A. Maher, and Changho Choi

Advanced Imaging Research Center, University of Texas Southwestern Medical Center, Dallas, Texas (V.T., Z.A., P.A., J.B., I.D., B.P.T., M.C.P., A.D.S., C.R.M., C.C.); Department of Pathology, University of Texas Southwestern Medical Center, Dallas, Texas (E.V.D., K.J.H., J.M.R.); Harold C. Simmons Cancer Center, University of Texas Southwestern Medical Center, Dallas, Texas (K.J.H., C.M.L., J.M.R., C.J.M., E.P, B.E.M., E.A.M., C.C.); Annette Strauss Center for Neuro-Oncology, University of Texas Southwestern Medical Center, Dallas, Texas (K.J.H., J.M.R., C.J.M., B.E.M., E.A.M.); Department of Clinical Sciences, University of Texas Southwestern Medical Center, Dallas, Texas (A.G., S.Z.); Philips Healthcare, Andover, Massachusetts (S.K.G.); Department of Radiology, University of Texas Southwestern Medical Center, Dallas, Texas (S.K.G., M.C.P., A.D.S., C.R.M., C.C.); Department of Neurological Surgery, University of Texas Southwestern Medical Center, Dallas, Texas (M.L., C.J.M., E.P, T.R.P., B.E.M.); Philips Medical Systems, Cleveland, Ohio (I.D.); Department of Neurology and Neurotherapeutics, University of Texas Southwestern Medical Center, Dallas, Texas (E.P, T.R.P., E.A.M.); Department of Radiation Oncology, University of Texas Southwestern Medical Center, Dallas, Texas (T.R.P.); Howard Hughes Medical Institute, University of Texas Southwestern Medical Center, Dallas, Texas (R.J.D.); Children's Research Institute, University of Texas Southwestern Medical Center, Dallas, Texas (R.J.D.); McDermott Center for Human Growth and Development, University of Texas Southwestern Medical Center, Dallas, Texas (R.J.D.); Department of Pediatrics, University of Texas Southwestern Medical Center, Dallas, Texas (R.J.D.); Department of Chemistry, University of Texas at Dallas, Dallas, Texas (A.D.S.); Department of Internal Medicine, University of Texas Southwestern Medical Center, Dallas, Texas (C.R.M., E.A.M.); Veterans Affairs North Texas Health Care System, Dallas, Texas (C.R.M.)

Corresponding Authors: Elizabeth A. Maher (Elizabeth.Maher@utsouthwestern.edu) and Changho Choi (Changho.Choi@utsouthwestern.edu), University of Texas Southwestern Medical Center, Dallas, TX.
*Present affiliation: Centre for Brain Research, Indian Institute of Science, Bangalore, India.

Abstract

Background. High-grade gliomas likely remodel the metabolic machinery to meet the increased demands for amino acids and nucleotides during rapid cell proliferation. Glycine, a non-essential amino acid and intermediate of nucleotide biosynthesis, may increase with proliferation. Non-invasive measurement of glycine by magnetic resonance spectroscopy (MRS) was evaluated as an imaging biomarker for assessment of tumor aggressiveness.

Methods. We measured glycine, 2-hydroxyglutarate (2HG), and other tumor-related metabolites in 35 glioma patients using an MRS sequence tailored for co-detection of glycine and 2HG in gadolinium-enhancing and non-enhancing tumor regions on 3T MRI. Glycine and 2HG concentrations as measured by MRS were correlated with tumor cell proliferation (MIB-1 labeling index), expression of mitochondrial serine hydroxymethyltransferase (SHMT2), and glycine decarboxylase (GLDC) enzymes, and patient overall survival.

Results. Elevated glycine was strongly associated with presence of gadolinium enhancement, indicating more rapidly proliferative disease. Glycine concentration was positively correlated with MIB-1, and levels higher than 2.5 mM showed significant association with shorter patient survival, irrespective of isocitrate dehydrogenase status. Concentration of 2HG did not correlate with MIB-1 index. A high glycine/2HG concentration ratio, >2.5, was strongly associated with shorter survival ($P < 0.0001$). GLDC and SHMT2 expression were detectable in all tumors with glycine concentration, demonstrating an inverse correlation with GLDC.

Conclusions. The data suggest that aggressive gliomas reprogram glycine-mediated one-carbon metabolism to meet the biosynthetic demands for rapid cell proliferation. MRS evaluation of glycine provides a non-invasive metabolic imaging biomarker that is predictive of tumor progression and clinical outcome.

Key Points

1. Glycine and 2-hydroxyglutarate in glioma patients are precisely co-detected using MRS at 3T.

2. Tumors with elevated glycine proliferate and progress rapidly.

3. A high glycine/2HG ratio is predictive of shortened patient survival.

Importance of the Study

Reprogramming of glycine metabolism to enhance glycine synthesis and consumption for increased nucleotide biosynthesis may be a strategy employed by rapidly proliferating gliomas. Beyond an assessment of gadolinium enhancement on MRI, a hallmark of high-grade disease, all other assessments of mutational status and markers of tumor aggressiveness require histological analysis. This study provides a non-invasive MR spectroscopic method to evaluate glycine and 2HG and correlate levels with clinical indicators of aggressiveness and glycine metabolism–associated enzymes. We show that in vivo quantitation of glycine may stratify glioma patients into prognostic groups and demonstrate for the first time that combined assessment of glycine and 2HG by MRS strongly predicts survival. The data suggest that in vivo assessment of glycine by MRS could be a valuable tool in the clinical management of gliomas, both in terms of identifying transformation from a slow-growing to highly proliferative tumor and in terms of being a survival predictor.

Cancer cells undergo metabolic reprogramming to support rapid cell proliferation and cell survival in the tumor microenvironment.[1,2] A recent focus in studies of glioma metabolism has been better understanding of the gain-of-function mutation in isocitrate dehydrogenase (IDH)[3–5] and the resulting production of 2-hydroxyglutarate (2HG).[6] Tumors also remodel the metabolic machinery to enhance synthesis of normal biomolecules such as amino acids and nucleotides via one-carbon metabolism, as needed for cell proliferation. An analysis of gene expression and nutrient consumption in the NCI-60 panel of cancer cell lines indicated that rates of glycine consumption and expression of glycine biosynthesis enzymes were elevated in highly proliferative cells.[7] Synthesis of glycine from serine via mitochondrial serine hydroxymethyltransferase (SHMT2) involves the transfer of a single carbon to 5,10-methylenetetrahydrofolate for nucleotide biosynthesis[8–10] (Supplementary Figure 1). Cleavage of glycine by glycine decarboxylase (GLDC) also provides a single carbon needed for nucleotide biosynthesis, in addition to direct incorporation of glycine in the purine ring.[7] Elucidating the role of glycine metabolism in patients with gliomas in vivo may provide clinical and biological insights for better understanding of cancer-associated metabolic rearrangements.

Development of a non-invasive tool to evaluate cancer-specific metabolic reprogramming in vivo and establishing its association with cellular, genetic, and enzymatic changes in gliomas will improve the clinical management of gliomas. We and others have reported elevated glycine levels in patients with high-grade gliomas using in vivo ^{1}H magnetic resonance spectroscopy (MRS).[11–16] Prior molecular studies using cell culture have shown that SHMT2 and GLDC expression is associated with tumor cell proliferation in breast cancers and with cell survival in ischemic regions of brain cancers.[7,17] A question remains as to whether alterations in mitochondrial enzymes associated with glycine metabolism correlate with characteristics of high-grade disease in glioma or the glycine pool is associated with proliferative capacity of the tumor and may predict patient survival. In this study, we conducted non-invasive measurements of glycine, 2HG, and other tumor-related metabolites in 35 glioma patients using point-resolved spectroscopy (PRESS) optimized for precise co-detection of glycine and 2HG. The biological and clinical relevance of the alterations in concentrations of glycine and 2HG was investigated by examining their association with blood–brain barrier breakdown as assessed by post-gadolinium enhancement on MRI, cell proliferation rate (MIB-1 labeling index), immunohistochemistry (IHC) of SHMT2 and GLDC enzymes, and overall survival. All tumors with elevated glycine showed post-contrast enhancement, high MIB-1 labeling index, and shortened survival, indicating high clinical relevance of glycine in gliomas. Our data suggest that glycine plays a key role in tumor cell proliferation and may serve as an important metabolic biomarker for clinical management of gliomas.

Materials and Methods

Patient Enrollment

Adult patients with gliomas were prospectively consented and enrolled into an institutional review board–approved research MRS imaging study at University of Texas Southwestern Medical Center over the past 10 years. For the current study, we selected 35 patients whose MR spectra were of sufficient quality for glycine analysis and who had available complete clinical information, including survival data, clinical scans (MRI with and without gadolinium) at the same time point, and, in 25 cases, sufficient tumor tissue for MIB-1 and enzyme expression analysis. Fifteen patients had non-enhancing tumors and 20 patients had enhancing tumors, none of which had a necrotic center. Demographic characteristics and metabolic and IHC details are listed in Table 1. Each patient had routine clinical MRI every 2–3 months with and without gadolinium. MRS was performed in each patient prior to treatment with chemotherapy or radiation. No patient had received bevacizumab or corticosteroids. Overall survival was obtained from clinical record review, and MIB-1 was performed as part of routine clinical histological assessment.

Magnetic Resonance Data Acquisition

Proton (^{1}H) MR experiments were carried out on a whole-body 3T scanner (Philips Medical Systems). Following survey imaging, T2–fluid attenuated inversion recovery (FLAIR) was acquired for tumor identification (repetition time [TR]/echo time [TE]/inversion time [TI] = 9000/125/2600 ms; field of view = 230 × 200 mm^2; slice thickness = 4 mm; 45 transverse slices). Single-voxel localized MRS was obtained with TE 97 ms PRESS (90°–180° pulse interval 16 ms), which had a 9.8 ms 90° pulse (bandwidth 4.2 kHz) and a 13.2 ms 180° radiofrequency (RF) pulse (bandwidth 1.3 kHz) at an RF field intensity (B_1) of 13.5 µT.[18,19] MRS was conducted more than 6 hours after the clinical MRI scan, when done on the same day, to avoid potential effects of gadolinium on MRS. The voxel for spectroscopy was positioned within the enhancing mass on post-contrast MRI when applicable, and within the T2-FLAIR hyperintensity region in non-enhancing scans, with care taken to avoid cystic, edematous, and/or necrotic regions. MRS was acquired from more than one location when the lesion was sufficiently large. MRS acquisition parameters included a sweep width of 2500 Hz, 2048 sampling points, and a TR of 2 s. The number of signal averages was 128–512, depending on the voxel size (4–8 mL). An unsuppressed water signal was acquired with TR 20 s and TE 14 ms for use as reference in metabolite quantification. Computer simulations were conducted to calculate the glycine and myo-inositol signals of PRESS TE 30 and 97 ms, using product-operator based density-matrix simulations that incorporated the volume selective RF and gradient pulses.[18,20] The spectra were broadened to singlet linewidth of 5 Hz, ignoring T$_2$ relaxation effects. In vitro test of PRESS TE 97 ms was conducted on a spherical-phantom solution (pH 7.0; temperature 37°C) with myo-inositol (20 mM) and N-acetylaspartate (10 mM).

Magnetic Resonance Data Processing

MRI data were processed using the vendor-supplied algorithms. For MRS, when spectra were acquired from multiple locations in a patient, one spectrum was selected, prior to subsequent analysis, by experienced MR spectroscopists (V.T. and C.C.) using the following criteria: (i) for a tumor having both enhancing and non-enhancing volumes, the spectrum from the enhancing region was chosen; and (ii) for a non-enhancing tumor, a spectrum with higher quality (ie, smaller linewidth and higher signal-to-noise ratio) was chosen. Spectra were apodized with a 1 Hz exponential function prior to Fourier transformation. Spectral fitting was performed, with LCModel software (v6.2F),[21] using basis spectra of 20 metabolites, which included glycine (Gly), 2HG, myo-inositol (mIns), glutamate (Glu), glutamine, γ-aminobutyric acid, lactate, threonine, citrate, glutathione, alanine, aspartate, ethanolamine, phosphoethanolamine, scyllo-inositol, taurine, glucose, Cho (glycerophosphocholine + phosphocholine), NAA (N-acetylaspartate + N-acetylaspartylglutamate), and Cr (creatine + phosphocreatine). The basis spectra were numerically calculated with density-matrix simulations. The basis signals of lipids and macromolecules were created using LCModel built-in functions. The millimolar concentrations of metabolites were quantified with reference to water at 45 M. MRS analysis was blinded to tumor biopsy analysis.

Biopsy Analysis for MIB-1 Labeling Index, and Enzymatic Expression of SHMT2 and GLDC

Formalin-fixed, paraffin-embedded tumor tissue from surgical resections was available for 26 patients. MIB-1 labeling was performed in 26 patients and expression of SHMT2 and GLDC was measured in 25 patients. Hematoxylin and eosin stained sections were reviewed, and representative slides (one slide for each tumor) were selected for IHC studies. The MIB-1 labeling index was determined using IHC staining with a monoclonal mouse antibody to MIB-1 (Dako) diluted 1:80 after heat-induced epitope retrieval using cell conditioning solution 1 (Ventana), a Tris-based buffer at pH of 8–8.5. IHC was performed on Ventana Benchmark Ultra automated stainer, using a Ventana Ultra-View Universal DAB Detection Kit. The MIB-1 labeling index was determined by manual morphometry using the Glasgow cell counting graticule.[22] The number of nuclei staining for MIB-1 relative to the total number of tumor nuclei was reported as MIB-1 labeling index. The expression of the mitochondrial enzymes SHMT2 and GLDC was measured in tumor tissues using IHC with rabbit polyclonal antibodies to SHMT2 (Sigma-Aldrich #HPA020549) and GLDC (Sigma-Aldrich #HPA002318), respectively, as previously described.[17] Briefly, the slides were baked for 20 minutes at 60°C followed by deparaffinization and hydration before the antigen retrieval. Heat-induced antigen retrieval was performed at pH 6.0 for 20 minutes in a Dako PT Link. The tissues were incubated with a peroxidase block followed by 20 minute incubation with the antibodies against SHMT2 and GLDC (1:250 for SHMT2 and 1:125 for GLDC) on a Dako Autostainer Link 48 system. A 15-minute

Table 1 Patient demographic and pathologic details

Patient ID	Sex	Age, y	Post-contrast MRI	Tumor Type	IDH Mutation	Survival Length, mo[††]	MIB-1, SHMT2, GLDC
P1	F	43	NE	AC	IDH1	17.1 (C)	Yes, Yes, Yes
P2	M	34	NE	O	IDH1	10.7 (C)	Yes, Yes, Yes
P3	M	30	NE	A	IDH1	114.8 (C)	Yes, Yes, Yes
P4	F	54	NE	A	Wildtype	56.6	Yes, No, No[†]
P5	F	25	NE	AA	IDH1	53.6 (C)	Yes, Yes, Yes
P6	M	41	NE	AA	Wildtype	66.2 (C)	Yes, Yes, Yes
P7	F	29	NE	A	IDH1	4.1 (C)	Yes, Yes, Yes
P8	F	21	NE	Glioma(R)	Not tested*	89.2 (C)	No, No, No*
P9	M	27	NE	AA	IDH1	75.7 (C)	Yes, Yes, Yes
P10	F	36	NE	AA	IDH1	16.2	Yes, Yes, Yes
P11	M	39	NE	A	IDH1	34 (C)	Yes, Yes, Yes
P12	F	30	NE	O	IDH2	19 (C)	No, No, No#
P13	M	43	NE	AA	IDH1	65.7 (C)	Yes, Yes, Yes
P14	M	59	NE	Glioma(R)	Not tested*	30.1 (C)	No, No, No*
P15	F	33	NE	Glioma(R)	Not tested*	8.8	No, No, No*
P16	F	25	E	GBM	Wildtype	12.9 (C)	Yes, Yes, Yes
P17	M	37	E	GBM	IDH1	16.4 (C)	Yes, Yes, Yes
P18	M	59	E	GBM	Wildtype	0.8	Yes, Yes, Yes
P19	F	69	E	GBM(R)	Widltype	4.8	No, No, No#
P20	F	48	E	AA	IDH1	4.9	No, No, No#
P21	F	48	E	AO	IDH2	46.4 (C)	Yes, Yes, Yes
P22	F	79	E	GBM(R)	Not tested*	4.0	No, No, No#
P23	M	69	E	GBM	Wildtype	7.9	Yes, Yes, Yes
P24	M	38	E	O	IDH1	70.1 (C)	No, No, No#
P25	M	38	E	GBM	IDH1	6.1	Yes, Yes, Yes
P26	M	27	E	AO	IDH1	63.2 (C)	Yes, Yes, Yes
P27	M	38	E	AO	IDH1	45.1	Yes, Yes, Yes
P28	F	54	E	AO	IDH1	42.8 (C)	Yes, Yes, Yes
P29	F	46	E	AO	IDH1	40.4 (C)	Yes, Yes, Yes
P30	M	43	E	AO	IDH1	86.2 (C)	Yes, Yes, Yes
P31	M	22	E	GBM	Wildtype	19.2	No, No, No
P32	M	40	E	GBM	Wildtype	2.1	Yes, Yes, Yes
P33	M	54	E	AO	IDH1	99.9 (C)	Yes, Yes, Yes
P34	F	32	E	GBM	IDH1	5.4	Yes, Yes, Yes
P35	M	55	E	GBM	Wildtype	7.1	Yes, Yes, Yes

Ages are presented with respect to the MRS scan time points. The patient index is identical to those in Fig. 2D. Survival length was calculated from the time of MRS scan.
NE, post contrast non-enhancing; E, post contrast enhancing; A, astrocytoma; AA, anaplastic astrocytoma; O, oligodendroglioma; AO, anaplastic oligodendroglioma; GBM, glioblastoma; glioma (R), radiographically identified glioma; yes, test was conducted; no, test was not conducted. †IHC of SHMT2 and GLDC was not performed. *IDH status or IHC measurement was not performed (biopsy or surgery was not conducted). # Tissue was not available for IHC measurements. ††Survival lengths with (C) were censored in the Kaplan–Meier analysis.

rabbit linker (Dako K8009) incubation was performed for GLDC IHC. The antibody stains were visualized using the EnVision FLEX visualization system. The IHC scores for SHMT2 and GLDC were determined by multiplying staining intensity (range, 1–3) with the percentage of cells stained positively for the antibodies.

Statistical Analysis

Cramér–Rao lower bounds of MRS estimation of metabolites were obtained with LCModel built-in algorithm.[21] Pearson's correlation analysis was performed between metabolite estimates and IHC measurements. Student's

t-test was performed for group comparison of MRS and biopsy analyses. Kaplan–Meier analysis and log-rank test were performed to compare overall survival of patients for MRS and IHC measurements. Hazard ratios were estimated by Cox regression models. The survival time was defined as the time length from MRS scan date to date of death for MRS variables and from surgery date to date of death for IHC measurements, and censored at the end of the study. For each of the experimental variables, a cutoff value that achieved best separation in overall survival was determined. All estimates were presented as mean ± SD. Statistical analyses were performed using SAS 9.4.

Results

Validation of MRS for Detection of Glycine

Computer simulations indicated that TE 97 ms PRESS gave rise to approximately 4-fold reduction of the mIns signal at 3.55 parts per million (ppm) compared with TE 30 ms PRESS (J-coupling effects) and consequently the intensity of the mIns signal intensity became similar to the glycine signal at 3.55 ppm (Fig. 1A, B). An in vitro test of the TE 97 ms PRESS closely reproduced the mIns signal pattern predicted by the simulation (Fig. 1C). Calculated sum spectra of glycine and mIns (Fig. 1D) showed that, with increasing glycine-to-mIns concentration ratio, the composite signal at 3.55 ppm was noticeably altered while the mIns signal at 3.64 ppm remains clearly discernible, suggesting that the glycine and mIns signals in human brain can be reliably decomposed by spectral fitting. In vivo spectra from a tumor and normal-appearing contralateral brain in a glioma patient, obtained with TE 97 ms PRESS, showed well-resolved metabolite signals on a relatively flat spectral baseline. The spectrum from the contralateral brain showed the expected healthy brain pattern of a glycine plus mIns composite signal between 3.5 and 3.7 ppm, giving a glycine estimate of 0.4 mM, but the spectrum from the tumor showed an altered composite signal pattern wherein the peak at 3.55 ppm was clearly larger than the signal at 3.64 ppm, indicating elevation of glycine (Figs. 1E, F). Glycine was estimated to be 1.5 mM for the tumor. In the tumor spectrum, a 2HG signal at 2.25 ppm was clearly resolved from the adjacent signals of glutamate and glutamine, which was achievable due to narrowing of the metabolite signals at the optimized TE.[18,19]

Glycine and Post-Gadolinium MRI

We evaluated glycine and 2HG in 35 patients with gliomas, of which 15 were non-enhancing and 20 were enhancing at the time of MRS. Representative spectra are shown in Fig. 2. For an IDH-mutant non-enhancing tumor with low MIB-1, a 2HG signal was clearly discernible at 2.25 ppm and a low level of glycine was estimated (Fig. 2A). In contrast, 2 tumors with gadolinium enhancement and high MIB-1 showed much higher glycine levels (Fig. 2B, C). Level of 2HG was present in the IDH-mutant tumor (Fig. 2C). IHC for SHMT2 and GLDC demonstrated positive staining in all 3 tumors (Fig. 2A–C). When assessed in all tumors, glycine concentration was low in 14 of the 15 non-enhancing tumors (0.3–0.7 mM) (Fig. 2D). In contrast, glycine was substantially elevated in all 20 enhancing tumors, with levels ranging from 2 to 7.5 mM. The mean glycine concentration was significantly higher in enhancing tumors than in non-enhancing tumors (Fig. 2E), possibly indicating an increase in the glycine pool associated with breakdown of the blood–brain barrier and more rapidly proliferating tumor. This relationship was supported by data from 2 tumors with both enhancing and non-enhancing regions (P22 and P29), which showed that glycine was distinctly higher in the enhancing region (Supplementary Figure 2). Concentration of 2HG was significantly higher in the IDH-mutant tumors compared with the IDH-wildtype tumors, while there was no significant association of glycine concentration with IDH mutation (Fig. 2D, E).

Glycine and Immunohistochemistry

Of the 35 patients in Fig. 2D, MIB-1 labeling index was measured in 26. It was approximately 5-fold higher in enhancing than in non-enhancing tumors (Fig. 3A), consistent with established association of high cellular proliferation in regions of gadolinium enhancement on clinical MRI of gliomas. Since the blood–brain barrier breakdown may be a consequence of rapid tumor cell proliferation, we performed a correlative analysis of glycine concentration and MIB-1. A significant positive correlation was observed (Fig. 3B). Immunohistochemistry of tumor biopsies showed significant expression of SHMT2 and GLDC in all 25 tumors (IHC scores of 5–300 for SHMT2 and 20–300 for GLDC), as previously shown.[17] The mean SHMT2 expression was not significantly different between enhancing and non-enhancing gliomas (Fig. 3C), and glycine concentration was not significantly correlated with SHMT2 expression (Fig. 3D). While GLDC expression was not significantly different between enhancing and non-enhancing gliomas (Fig. 3E), a significant inverse correlation between glycine concentration and GLDC expression was observed (Fig. 3F). There was no significant correlation between 2HG level and MIB-1 (Fig. 3G) or between glycine and 2HG concentrations (Fig. 3H). MIB-1 labeling index was not significantly correlated with SHMT2 expression but showed a significant inverse correlation with GLDC expression (Supplementary Figure 3).

Glycine Associated with Tumor Progression

Two brainstem glioma patients were included in the study. Patient (P)15 presented with high glycine without measurable 2HG (Fig. 4A) and experienced steady worsening of clinical symptoms despite aggressive treatment with the development of post-contrast enhancement within 6 months after the MRS. In contrast, P8 had low glycine concentration with elevated 2HG at the time of presentation (Fig. 4B) and had stable, non-enhancing clinical MRI for the subsequent 7 years of follow-up after the MRS. Repeat post-contrast MRI in 4 additional patients showed close association of elevated glycine with rapid tumor progression (Fig. 4C). Irrespective of the IDH mutation and 2HG concentration, the tumors with high glycine levels
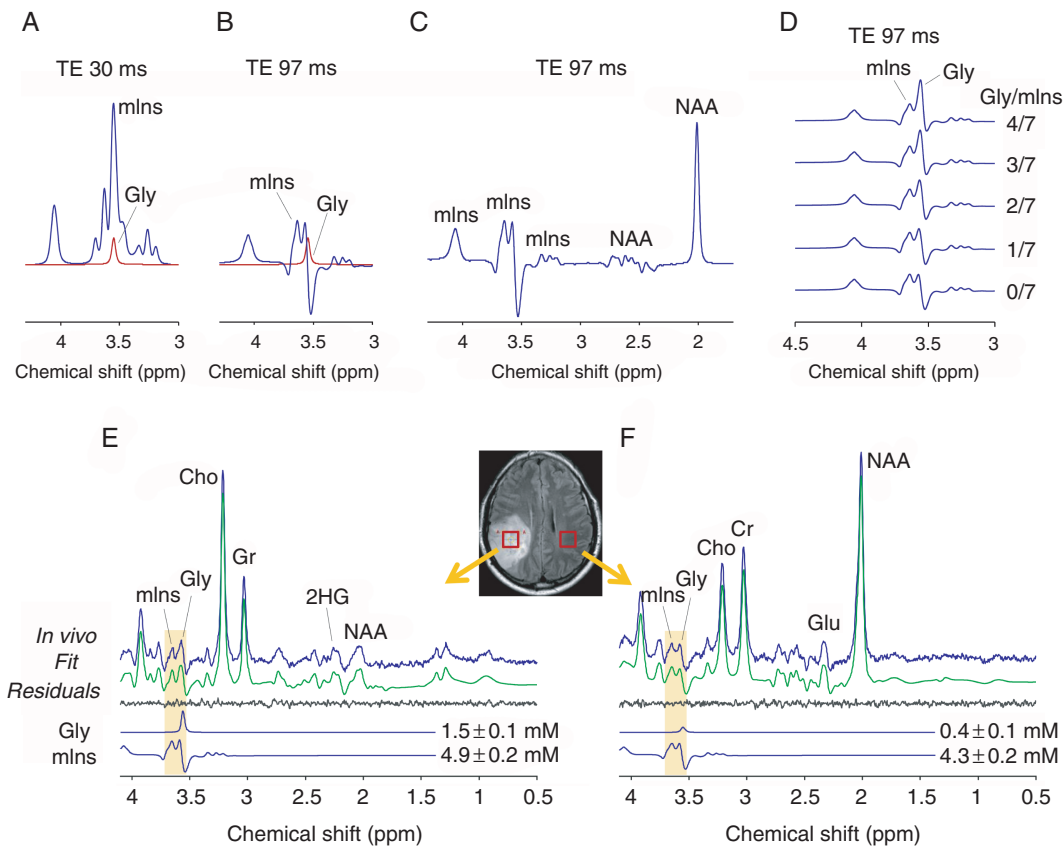
Fig. 1 Illustration of optimized MRS for detection of glycine in the human brain at 3T. (A, B) ^{1}H MR spectra of glycine (Gly) and myo-inositol (mIns), numerically calculated for PRESS echo time (TE) 30 ms and optimized PRESS TE 97 ms, are presented for a Gly-to-mIns concentration ratio of 1/7 (in vivo concentration ratio of the metabolites in the healthy brain[15]). (C) An in vitro TE 97 ms PRESS spectrum of mIns is presented for comparison with the theoretical signal pattern of mIns. (D) Sum spectra of Gly and mIns, calculated with PRESS TE 97 ms, for their concentration ratios of 0, 1/7, 2/7, 3/7 and 4/7. (E, F) Representative in vivo PRESS TE 97 ms spectra from a tumor mass and a contralateral brain in a subject with IDH1-mutated anaplastic oligodendroglioma are presented together with spectral fitting outputs, signals of Gly and mIns, and voxel positioning in an axial T2-FLAIR image. The millimolar concentrations of Gly and mIns are shown with standard deviations. The voxel size and scan time were 8 mL and 4.3 min in both scans (128 averages with TR 2 s). The spectra were scaled with respect to the water signals from individual voxels. Cho, choline; Cr, creatine; NAA, N-acetylaspartate; Glu, glutamate.

underwent rapid progression. The T2-FLAIR hyperintensity and post-contrast enhancing regions in each scan were increased by 4- to 5-fold in 3 directions within 1–4 months of their first MRI scans.

Survival Analyses of Glycine and 2HG

To determine whether overall survival was associated with glycine concentration, we performed Kaplan–Meier analysis. Survival was significantly shorter in patients with glycine concentration higher than 2.5 mM compared with those with less than 2.5 mM ($P = 0.003$) (Fig. 5A, Supplementary Table 1). The hazard ratio of the high glycine tumors with respect to the low-glycine tumors was 6.8. In contrast, and consistent with published literature, higher risk of death was associated with lower concentrations of 2HG (Fig. 5B) and lack of IDH mutation. For this study, we used 1 mM for this analysis, since this was

the detection threshold in our prior 2HG MRS study.[23] Patients with lower than 1 mM 2HG showed significantly shorter survival than those with higher than 1 mM 2HG ($P = 0.01$). The hazard ratio of the poor-survival group relative to the long-survival group was smaller in 2HG compared with glycine (3.8 vs 6.8). Since high glycine and low 2HG were associated with poor survival, we tested the glycine/2HG concentration ratio for a poor-survival predictor. Estimates of 2HG <1 mM were set to unity in the analysis. Compared with glycine alone, the glycine/2HG ratio showed much stronger association with survival. Glycine/2HG greater than 2.5 was significantly associated with shorter survival ($P < 0.0001$, hazard ratio 20, median survival 5.4 mo). MIB-1 labeling index of 10% was significantly associated with survival (Fig. 5D), in agreement with prior reports of high MIB-1 and shorter survival in glioma.[24–26] While SHMT2 did not show significant association with survival (Fig. 5E), GLDC expression did associate with survival (Fig. 5F).
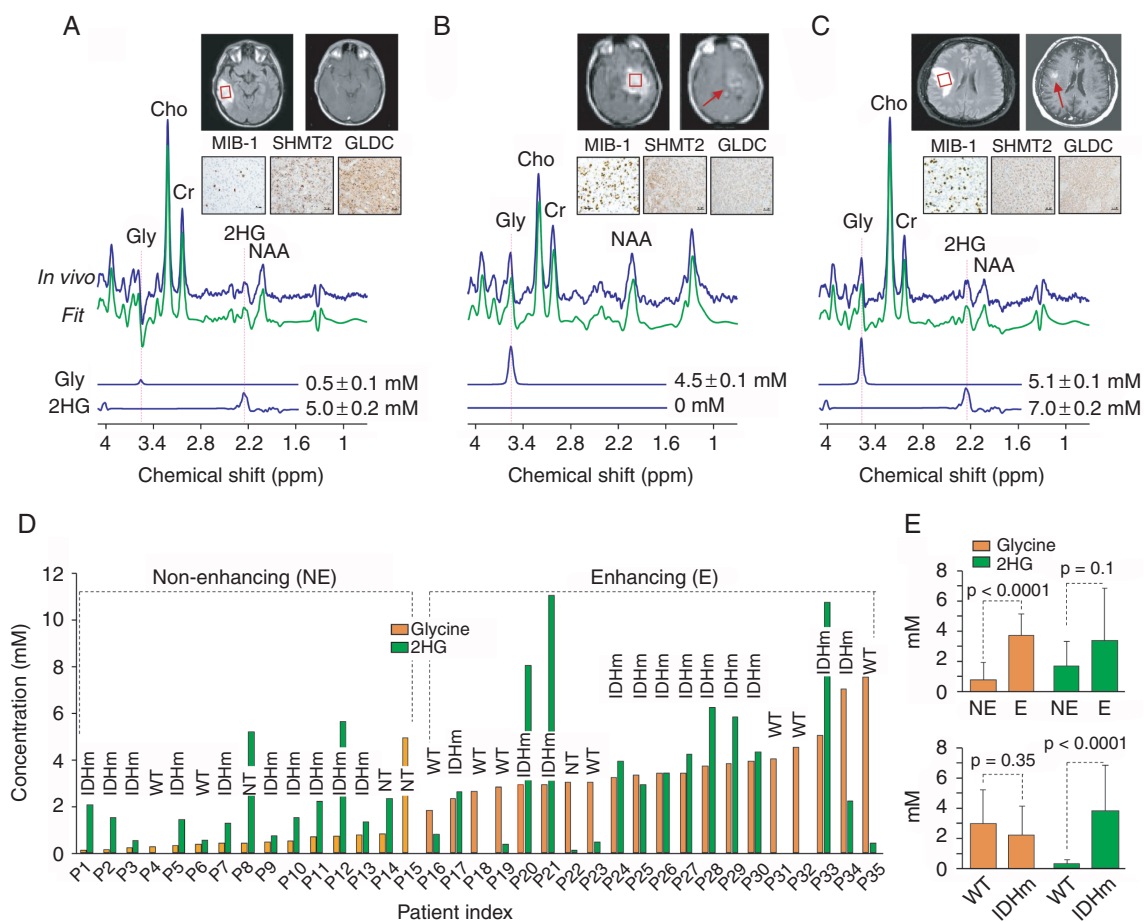
Fig. 2 Representative ¹H spectra from glioma patients, together with MRI and IHC, and association of glycine levels with the post-contrast enhancement status. (A–C) In vivo ¹H spectra from 3 glioma patients are presented together with the glycine and 2HG signal estimates, T2-FLAIR imaging, post-contrast MRI, and IHC analyses of the tumor biopsies for cell proliferation rate (MIB-1) and expressions of SHMT2 and GLDC enzymes. The tumor type is (from left to right) IDH-mutated non-enhancing anaplastic astrocytoma (IDH1 R132H), IDH-wildtype enhancing glioblastoma, and IDH-mutated enhancing anaplastic oligodendroglioma (IDH1 R132H). The MRS voxels are shown in T2-FLAIR images. The spectra were scaled with respect to the water signals from individual voxels. Vertical dotted lines are drawn at 3.55 and 2.25 ppm. (D) Estimates of glycine and 2HG are presented for 35 glioma patients, which included 15 patients with non-enhancing tumors (patient index P1–P15) and 20 patients with enhancing tumors (P16–P35). Patients were indexed in the ascending order of glycine estimation for each of the non-enhancing (NE) and enhancing (E) tumor groups. IDHm, IDH mutated (N = 22); WT, IDH wildtype (N = 9); NT, not tested for IDH status (N = 4). (E) The mean glycine and 2HG concentrations are bar graphed for the non-enhancing and enhancing tumor groups and for IDH mutated and IDH-wildtype tumor groups. Error bars represent standard deviation.

Discussion and Conclusion

We found that elevated concentration of glycine in gliomas is closely associated with rapid cell proliferation and post-contrast enhancement, indicative of aggressive disease. It is very unlikely that the high glycine levels in the post-contrast enhancing tumors were due to contamination by blood or cerebrospinal fluid, since glycine levels are very low in both (<0.5 mM).[27,28] Our observation of glycine concentration being significantly correlative with both post-gadolinium enhancement and MIB-1 labeling index suggests that aggressively proliferating tumors

remodel glycine synthesis and consumption. As such, a non-invasive method to assess glycine concentration may provide a significant imaging biomarker of cell proliferation in gliomas and subsequent response to treatment. Importantly, the brainstem tumor that was non-enhancing at the time of MRS detection of elevated glycine underwent progression shortly after and showed post-contrast enhancement at later time points. This observation suggests that alteration in glycine metabolism may precede blood–brain barrier breakdown, and thus elevation of glycine could potentially serve as an early imaging biomarker predictive of high-grade transformation. MRS monitoring of glycine in the brainstem or deep brain regions may
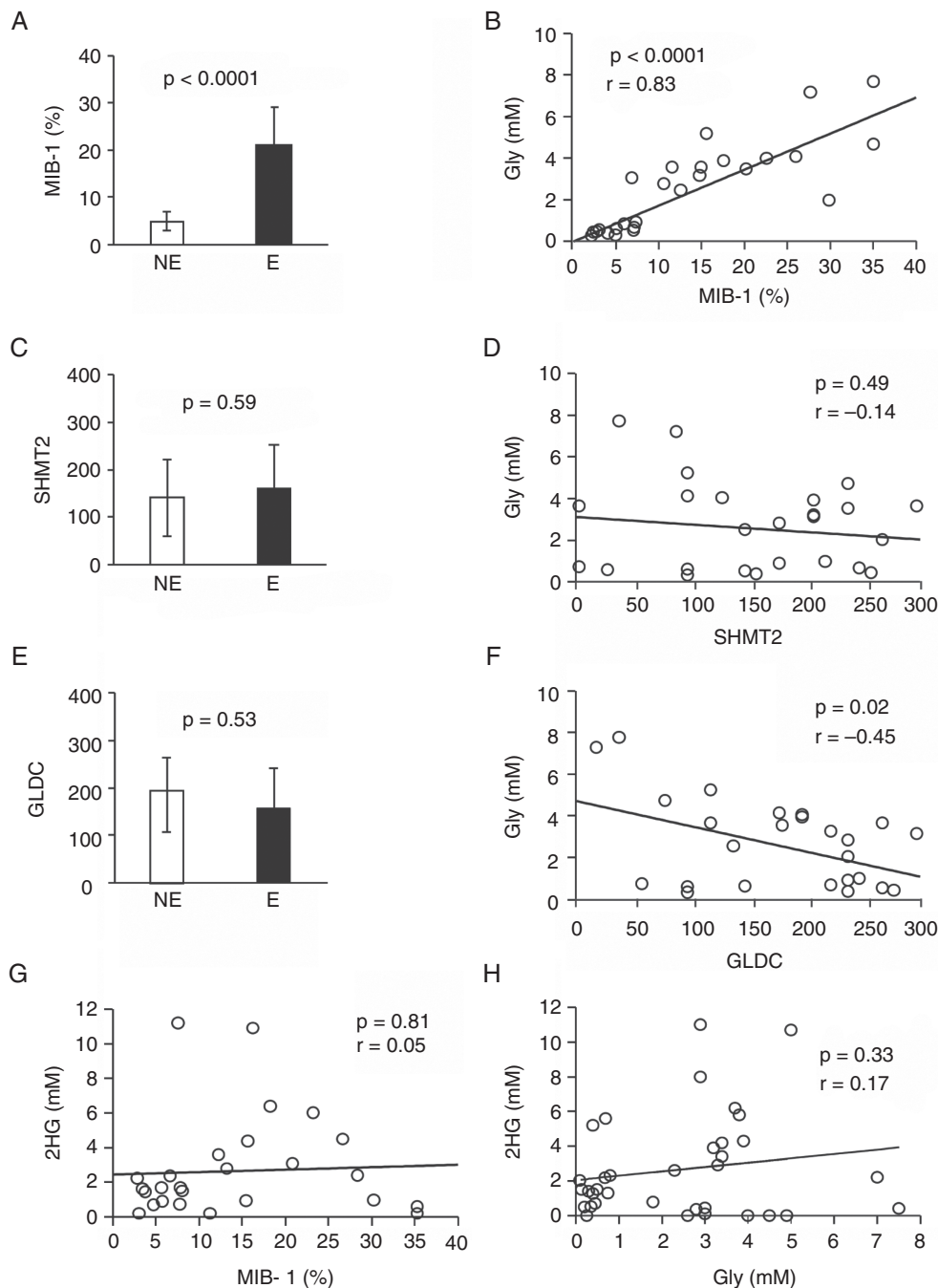
Fig. 3 Comparison between MRS, tumor tissue analysis, and post-contrast MRI. (A) Comparison of the mean MIB-1 labeling index between 11 non-enhancing (NE) and 15 enhancing (E) tumors. Error bars denote standard deviation. (B) Correlation plot between MIB-1 and glycine levels in the 26 patients. (C) Comparison of the mean IHC score of SHMT2 expression between 10 non-enhancing and 15 enhancing tumors. (D) A correlation plot between SHMT2 IHC score and glycine levels in the 25 patients. (E) Comparison of mean score of GLDC expression between 10 non-enhancing and 15 enhancing tumors. (F) Correlation plot for GLDC and glycine in the 25 patients. (G) Correlation plot between 2HG and MIB-1 in 26 glioma patients. (H) Correlation plot between 2HG and glycine in 35 patients.

provide a particularly significant clinical value, since surgical intervention of brainstem and deep brain lesions carries high risk of permanent neurological deficits.

We also present here for the first time a strong association of elevated glycine with poor clinical outcome in

glioma patients. This was even more striking when presented as a ratio of glycine/2HG. In our overall survival analysis, low to undetectable 2HG in IDH wildtype tumors was associated with poor patient outcomes, in complete agreement with the known survival advantage of IDH
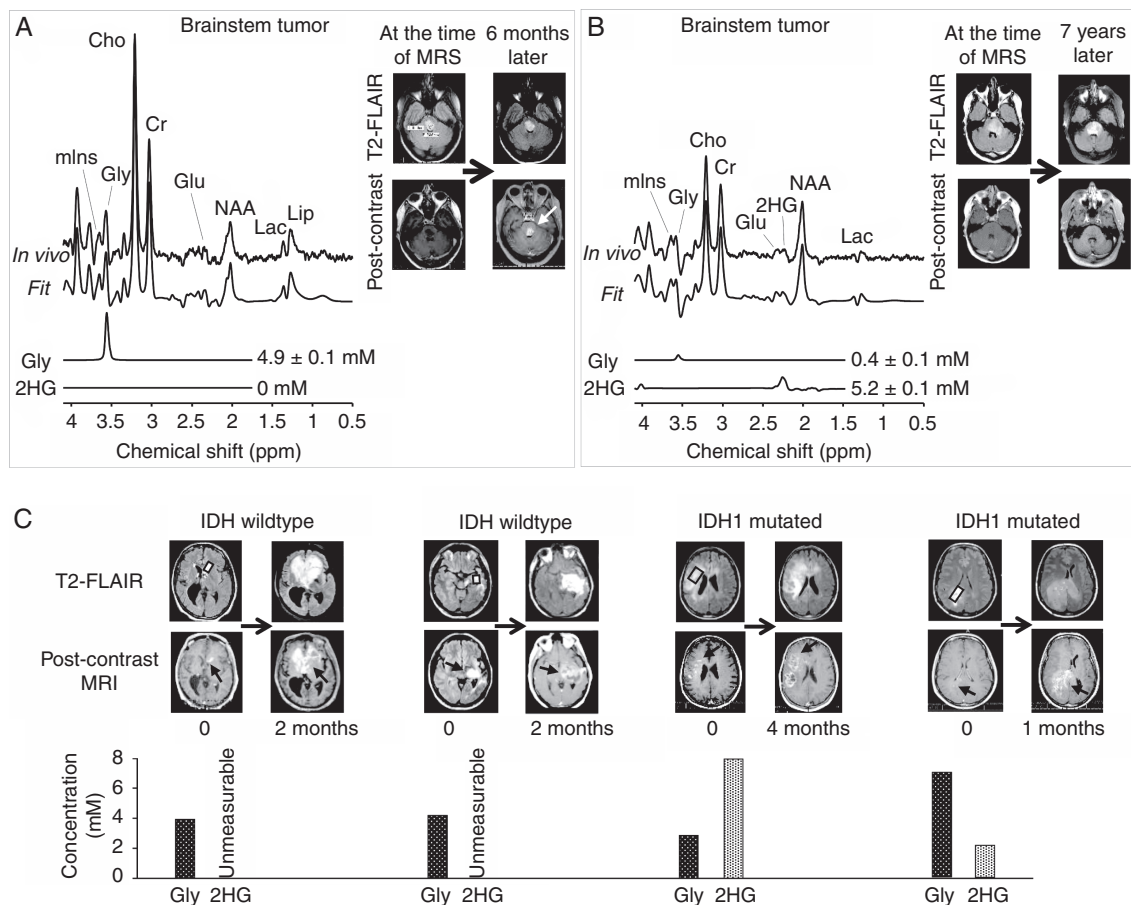
Fig. 4 Association of glycine and 2HG pool with tumor progression. (A, B) MRS data from 2 subjects with radiographically identified brainstem gliomas are presented together with T2-FLAIR and post-contrast MR images obtained at the time of MRS and at a later time point. (A) One tumor had highly elevated glycine and undetectable 2HG at the time of MRS (P15 in Fig. 2D) and showed enhancement on post-contrast MRI 6 months later. (B) The other tumor had low level of glycine and elevated 2HG at the time of MRS and remained non-enhancing for 7 years, without noticeable increase in the T2-FLAIR volume. (C) For each of 4 patients with enhancing gliomas, MRI data (T2-FLAIR and post-contrast MRI) at 2 time points are presented together with glycine and 2HG estimates obtained at the first MRI time point (0 mo). Data showed that tumors with elevated glycine progressed rapidly (1–4 mo), irrespective of IDH mutation.

mutation in glioma.[29,30] Interestingly, we found that high glycine concentration was more strongly associated with high risk of death than low 2HG and that the ratio of glycine to 2HG had the strongest separation between the groups. As we and others have previously shown, 2HG is an excellent imaging biomarker of IDH mutant gliomas[18,31,32] and 2HG MRS is being increasingly adopted as part of clinical MRI in many hospitals. Given the prognostic capability of 2HG, MRS monitoring of both glycine and 2HG may be useful for identifying aggressively proliferating tumors and predicting overall survival.

We observed a close link between glycine level and MIB-1 labeling index, which indicates association of elevated glycine with metabolic rearrangement in highly proliferating tumors. While a prior study demonstrated that an IDH-mutant expressing immortalized astrocytic cell line has a proliferative advantage over the same cells with

wildtype IDH,[33] our in vivo, non-invasive data in glioma patients did not show significant correlation of 2HG with MIB-1 cell proliferation index.

The expression of SHMT2 and GLDC was measurable in all tumors in this study, as in the study by Kim et al.[17] We found that SHMT2 expression and MIB-1 index were not significantly correlated, consistent with the prior report,[17] in which SHMT2 expression did not correlate with cell proliferation and viability in cultured cells. While SHMT2 expression was inversely correlated with survival in breast cancer patients in the Jain et al study,[7] our data did not show significant correlation between SHMT2 expression and overall survival in glioma patients. In our analysis, glycine levels, which showed strong correlation with tumor cell proliferation and malignant transformation, were not significantly correlated with SHMT2 expression. This result suggests
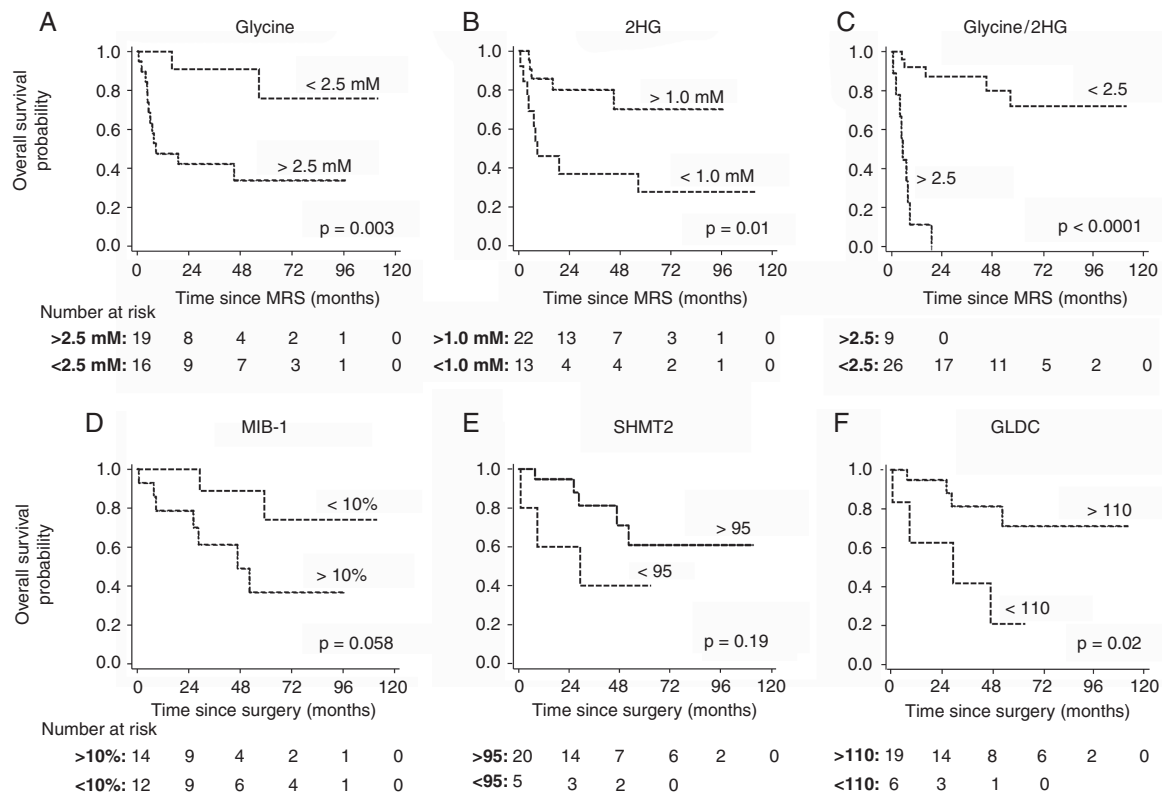
Fig. 5 Kaplan–Meier analyses of metabolite levels and enzymatic expression for overall survival of patients. The Kaplan–Meier survival analyses are presented for the MRS measurements of glycine (A), 2HG (B), and glycine-to-2HG ratio (C) and IHC analyses of MIB-1 labeling index (D) and expression of SHMT2 (E) and GLDC (F). The number of patients are 35 for glycine and 2HG, 26 for MIB-1, and 25 for SHMT2, and GLDC. The *P*-value represents the statistical significance of the difference in overall survival between 2 patient groups defined with a cutoff value that was responsible for the strongest statistical significance.

that, while tumors may have enhanced SHMT2 expression for glycine synthesis, glycine itself may be a predominant factor to identify a highly malignant tumor. SHMT2-mediated glycine synthesis may not be sufficient to meet the demands of glycine for nucleotide biosynthesis in rapidly proliferating tumor cells, and additional glycine requirement may be fulfilled from other sources, such as SHMT1-mediated glycine synthesis in cytosol and catalysis of sarcosine, choline, and threonine.[8,34]

Strong correlations of glycine with MIB-1 index and overall survival demonstrate that glycine level may reflect the proliferative and aggressive potential of the tumor cells more closely compared with histological measurements for expression of SHMT2 or GLDC enzymes. Increased cell proliferation in tumors with elevated glycine may be a combined result of SHMT2 and GLDC enzymatic activities. Cells with high glycine and relatively low expression of GLDC may have increased production of aminoacetone and methylglyoxal, which are toxic for the cells, as shown by Kim et al.[17] In our study, GLDC expression score less than 110 was associated with poor survival. Short survival in patients with low GLDC expression may

be a consequence of enhanced necrotic cell death resulting from increased production of toxic by-products amino acetone and methylglyoxal, in addition to concomitant cell proliferation.

There are several limitations in the present study. First, the number of patients enrolled is relatively small and we will validate the findings in a larger cohort where we have the power to analyze the non-enhancing and enhancing tumors as separate groups. This may identify even more refined subgroups where glycine or the glycine/2HG ratio is highly informative clinically. Second, approximately two thirds of the patients in the study were IDH mutated, with a mix of astrocytomas and oligodendrogliomas. Further study may be required to clarify the role of glycine according to individual glioma types, in particular in IDH-wildtype gliomas. Third, our overall survival analysis was performed without other factors taken into account, such as Karnofsky performance status, age, and O6-methylguanine-DNA methyltransferase promoter methylation status, which may be associated with patient survival.

In conclusion, the present study provides in vivo evidence establishing the association of glycine metabolism

with clinical features of tumor cell proliferation and aggressiveness in glioma. Close association of glycine level with MIB-1 suggests that gliomas may reprogram the glycine metabolism to drive the cellular and metabolic machinery to support the demands of rapid cell proliferation. Of major clinical significance would be the identification of a non-invasive imaging biomarker that would identify the transition from low- to high-grade disease and from posttreatment to recurrent disease. The ease of glycine measurement by MRS and the significant correlations with markers of tumor aggressiveness identified in this study suggest that glycine is a strong biomarker candidate for this important clinical need. Moreover, our observation that elevated glycine is predictive of poor patient outcome, even in IDH-mutant tumors, adds weight to its potential value in clinical imaging and glioma management.

Supplementary Material

Supplementary data are available at *Neuro-Oncology* online.

Keywords

gliomas | glycine | 2-hydroxyglutarate | magnetic resonance spectroscopy | one-carbon metabolism

References

1. Hanahan D, Weinberg RA. Hallmarks of cancer: the next generation. *Cell.* 2011;144(5):646–674.
2. DeBerardinis RJ, Thompson CB. Cellular metabolism and disease: what do metabolic outliers teach us? *Cell.* 2012;148(6):1132–1144.
3. Salamanca-Cardona L, Shah H, Poot AJ, et al. In vivo imaging of glutamine metabolism to the oncometabolite 2-hydroxyglutarate in IDH1/2 mutant tumors. *Cell Metab.* 2017;26(6):830–841.e3.
4. McBrayer SK, Mayers JR, DiNatale GJ, et al. Transaminase inhibition by 2-hydroxyglutarate impairs glutamate biosynthesis and redox homeostasis in glioma. *Cell.* 2018;175(1):101–116.e25.
5. Bunse L, Pusch S, Bunse T, et al. Suppression of antitumor T cell immunity by the oncometabolite (R)-2-hydroxyglutarate. *Nat Med.* 2018;24(8):1192–1203.
6. Dang L, White DW, Gross S, et al. Cancer-associated IDH1 mutations produce 2-hydroxyglutarate. *Nature.* 2009;462(7274):739–744.
7. Jain M, Nilsson R, Sharma S, et al. Metabolite profiling identifies a key role for glycine in rapid cancer cell proliferation. *Science.* 2012;336(6084):1040–1044.
8. Locasale JW. Serine, glycine and one-carbon units: cancer metabolism in full circle. *Nat Rev Cancer.* 2013;13(8):572–583.
9. Amelio I, Cutruzzolá F, Antonov A, Agostini M, Melino G. Serine and glycine metabolism in cancer. *Trends Biochem Sci.* 2014;39(4):191–198.
10. Newman AC, Maddocks ODK. One-carbon metabolism in cancer. *Br J Cancer.* 2017;116(12):1499–1504.
11. Hattingen E, Lanfermann H, Quick J, Franz K, Zanella FE, Pilatus U. 1H MR spectroscopic imaging with short and long echo time to discriminate glycine in glial tumours. *MAGMA.* 2009;22(1):33–41.
12. Choi C, Ganji SK, DeBerardinis RJ, et al. Measurement of glycine in the human brain in vivo by 1H-MRS at 3 T: application in brain tumors. *Magn Reson Med.* 2011;66(3):609–618.
13. Maudsley AA, Gupta RK, Stoyanova R, et al. Mapping of glycine distributions in gliomas. *AJNR Am J Neuroradiol.* 2014;35(6 Suppl):S31–S36.
14. Ganji SK, Maher EA, Choi C. In vivo (1)H MRSI of glycine in brain tumors at 3T. *Magn Reson Med.* 2016;75(1):52–62.
15. Tiwari V, An Z, Ganji SK, et al. Measurement of glycine in healthy and tumorous brain by triple-refocusing MRS at 3 T in vivo. *NMR Biomed.* 2017; 30:e3747. doi:10.1002/nbm.3747
16. Babourina-Brooks B, Kohe S, Gill SK, et al. Glycine: a non-invasive imaging biomarker to aid magnetic resonance spectroscopy in the prediction of survival in paediatric brain tumours. *Oncotarget.* 2018;9(27):18858–18868.
17. Kim D, Fiske BP, Birsoy K, et al. SHMT2 drives glioma cell survival in ischaemia but imposes a dependence on glycine clearance. *Nature.* 2015;520(7547):363–367.
18. Choi C, Ganji SK, DeBerardinis RJ, et al. 2-hydroxyglutarate detection by magnetic resonance spectroscopy in IDH-mutated patients with gliomas. *Nat Med.* 2012;18(4):624–629.

19. Choi C, Ganji S, Hulsey K, et al. A comparative study of short- and long-TE ¹H MRS at 3 T for in vivo detection of 2-hydroxyglutarate in brain tumors. *NMR Biomed.* 2013;26(10):1242–1250.

20. Thompson RB, Allen PS. Sources of variability in the response of coupled spins to the PRESS sequence and their potential impact on metabolite quantification. *Magn Reson Med.* 1999;41(6):1162–1169.

21. Provencher SW. Estimation of metabolite concentrations from localized in vivo proton NMR spectra. *Magn Reson Med.* 1993;30(6):672–679.

22. Daoud EV, Rajaram V, Cai C, et al. Adult brainstem gliomas with H3K27M mutation: radiology, pathology, and prognosis. *J Neuropathol Exp Neurol.* 2018;77(4):302–311.

23. Choi C, Raisanen JM, Ganji SK, et al. Prospective longitudinal analysis of 2-hydroxyglutarate magnetic resonance spectroscopy identifies broad clinical utility for the management of patients with IDH-mutant glioma. *J Clin Oncol.* 2016;34(33):4030–4039.

24. Thotakura M, Tirumalasetti N, Krishna R. Role of Ki-67 labeling index as an adjunct to the histopathological diagnosis and grading of astrocytomas. *J Cancer Res Ther.* 2014;10(3):641–645.

25. Zeng A, Hu Q, Liu Y, et al. IDH1/2 mutation status combined with Ki-67 labeling index defines distinct prognostic groups in glioma. *Oncotarget.* 2015;6(30):30232–30238.

26. Chen WJ, He DS, Tang RX, Ren FH, Chen G. Ki-67 is a valuable prognostic factor in gliomas: evidence from a systematic review and meta-analysis. *Asian Pac J Cancer Prev.* 2015;16(2):411–420.

27. Schmidt JA, Rinaldi S, Scalbert A, et al. Plasma concentrations and intakes of amino acids in male meat-eaters, fish-eaters, vegetarians and vegans: a cross-sectional analysis in the EPIC-Oxford cohort. *Eur J Clin Nutr.* 2016;70(3):306–312.

28. Batllori M, Casado M, Sierra C, et al. Effect of blood contamination of cerebrospinal fluid on amino acids, biogenic amines, pterins and vitamins. *Fluids Barriers CNS.* 2019;16(1):34.

29. Parsons DW, Jones S, Zhang X, et al. An integrated genomic analysis of human glioblastoma multiforme. *Science.* 2008;321(5897):1807–1812.

30. Yan H, Parsons DW, Jin G, et al. IDH1 and IDH2 mutations in gliomas. *N Engl J Med.* 2009;360(8):765–773.

31. Andronesi OC, Kim GS, Gerstner E, et al. Detection of 2-hydroxyglutarate in IDH-mutated glioma patients by in vivo spectral-editing and 2D correlation magnetic resonance spectroscopy. *Sci Transl Med.* 2012;4(116):116ra4.

32. Pope WB, Prins RM, Albert Thomas M, et al. Non-invasive detection of 2-hydroxyglutarate and other metabolites in IDH1 mutant glioma patients using magnetic resonance spectroscopy. *J Neurooncol.* 2012;107(1):197–205.

33. Koivunen P, Lee S, Duncan CG, et al. Transformation by the (R)-enantiomer of 2-hydroxyglutarate linked to EGLN activation. *Nature.* 2012;483(7390):484–488.

34. Meltzer HL, Sprinson DB. The synthesis of 4-C14, N15-L-threonine and a study of its metabolism. *J Biol Chem.* 1952;197(1):461–474.